Fuzzy Majority Voting-Based Fusion of Markovian Probability for Improved Land Cover Change Prediction: A Case Study of Delta, Egypt

Salah, M.
Department of Surveying Engineering, Faculty of Engineering Shoubra - Benha University, 108 Shoubra st., Cairo, Egypt, E-mail: engmod2000@yahoo.com

Abstract
This research predicts the future changes of Delta, Egypt using Landsat satellite images of 2002, 2010 and 2015 through the fusion of Markovian probability maps for improved land use/cover changes (LUCC). First, each of the three satellite images was radiometrically and atmospherically corrected. After that, two different classification algorithms were used to prepare the base maps for: 2002; 2010; and 2015, with three major classes: land areas; cultivated areas; and water bodies. The classifiers used include: Self-Organizing Map (SOM); and Classification Trees (CTs). A total of 6 uncorrelated feature attributes have been incorporated in the classification in order to mitigate the impacts of classification errors on change detection. The classified images of 2002 and 2010 were then used to predict the 2015 land use with a Markov Chain Model. As a result, two Markovian probability images were obtained, one for the SOM-based model and the other for the CTs one. The Fuzzy Majority Voting (FMV) was then applied for combining the two Markovian probability images. This would lead to an enhanced prediction of 2015 land use. At the end, the final predicted image for 2015 land use was validated with the 2015 classified image. Two stages of validation procedures were applied in this research: 1) the Kappa index of agreement (KIA) was used to validate the overall performance of the prediction process with the most accurate prediction of 0.8871 being achieved; 2) the components of agreement and disagreement were used to gain a detailed idea about the performance of the prediction process with agreement and disagreement of 82.13% and 17.87%, respectively, being achieved. On the other hand, the Markov model extrapolates that coastal area decreased from 35.80% to 35.30% of the total study area during 2002–2015. Finally and as compared with 2015, the prediction of 2050 land use shows 1.11% increase of water body.

1. Introduction and Previous Work

Remote sensing provides the privilege of rapid data acquisition and lower cost than ground techniques (Pal and Mather, 2004). Satellite images provide time series data of land use/cover which are useful to identify the changes and their impact on the environment. In remote sensing, change detection is the process of determining and monitoring the land cover changes in different time periods (Tewolde and Cabral, 2011). Present LUCC and the expected changes in the near future are of great important for planning and management. Therefore, it is important to monitor land use change within a certain period of time and predict patterns of future land use change. The issue is so important that scientists have formed an international organization, called "LUCC" which is connected with the International Human Dimensions of Global Change Program and the International Geosphere Biosphere Program (LUCC, 2002). It is estimated that 15% of the world's land has been destroyed by soil erosion (De Chazal and Rounsevell, 2009). Erosion of coastal areas is a major worldwide problem, particularly in vulnerable such as the northern coast of Egypt (Gaber et al., 2014). Acting together, erosion, sea-level rise and reduced sediment supply due to the closure of the High Aswan Dam in 1964 could potentially cause a relative rise in the sea level over the northeastern delta plain of approximately 1 m by the year 2100 (Stanley, 1988). This would submerge much of the delta in the eastern part to as far south as 30 km from the present coastline.

Over two million people would be forced to abandon their homes, 214,000 jobs would be lost and over US $35 billion in land value, property, and tourism. Income would also be lost as a direct result of a sea level rise of 50 cm (El Raey, 1997). Therefore, there is an urgent need to predict the future scenario of the Delta coastline position on a regular basis. The models available to predict land use changes have become increasingly complex in recent years. Despite their complexity, the predictive power of these models remains relatively

weak (Iacono et al., 2012). However it is difficult to conclude which one gives more accurate representation (Wu and Webster, 2000). Among the existing prediction methods, the commonly used models are: Cellular Automata Markov Model; Multi Layer Perceptron Markov Model; and the Markov Chain Model.

Simulation with Cellular Automata Markov Model is based on a matrix of Markov transition areas; transitional suitability images and a user defined contiguity filter. One major limitation of this model is that preparing a suitability map for each land cover type is difficult in terms of data and information availability and is not perfect always. On the other hand, each variable is usually connected with a criterion that indicates its importance in the simulation process. Decision makers have to decide, based on their knowledge, the relative importance of each criterion (Wu, 2002). This may become a source of uncertainties in the simulation process (Qiang and Lam, 2015). Multi Layer Perceptron Markov Model uses the back propagation (BP) algorithm. Back propagation involves two major steps, forward and backward propagation. One advantage of using MLP is its ability to model all the transitions at once. As well, MLP neural network is quite capable of modeling non-linear relationships (Eastman, 2009). On the other hand, several factors affect the capabilities of the neural network to generalize. These include: number of nodes; number of training samples and iterations; learning rate; and the momentum (Atkinson and Tatnall, 1997).

Markov chains, on the other hand, have been applied to urban land use dynamics since the 1970s as an alternative to the large-scale urban simulation models. Markov chain models have the ability to describe the complex and long-term LUCC in terms of simple transition probabilities that makes them attractive alternatives to more complex models (Iacono et al., 2012). In this respect, Markov Chain Model minimizes computation time and reduces memory requirements. As well, it needs no specified parameters which should be determined based on experience and the complexity of the landscapes. Markov assumes that the forces that produced the changes will continue to do so in the future (Clark labs, 2012). It is often desirable to use a yearly transition matrix in order to set the modeling step in one year. However, these yearly matrices do not necessary represent adequately the yearly transitions because the changes observed by comparison of the beginning and the end of the period are only a part of the changes which occurred (Mas and Vega, 2012). Many researches have been conducted to detect the LUCC overtime and predict the future scenario. As noted by Verburg et al., (2008), no single model is capable of considering all of the processes of LUCC at different scales. In many cases, it may be most appropriate to combine the outcomes of different models, which may lead to a better understanding of the LUCC change process (Castella et al., 2007). Joo et al., (2010) have used Landsat MSS and TM images to map land-use changes from the classified images of Seoul Metropolitan Area for the past 30 years. Spatio-temporal transition matrices were constructed from the classified images and applied into a Markov Chain based model to predict land-use changes for the study area. Wang and Mountrakis (2011) have integrated multiple neural networks to predict the urban growth of Denver Metropolitan Area, CO, USA. Bayes and Raquib (2012) predicted and analyzed the future urban growth of Dhaka City, Bangladesh, using the Landsat satellite images of 1989, 1999 and 2009. Three different models have been implemented to simulate the land cover map of 2009.

These models include: the Stochastic Markov Model, Cellular Automata Markov Model and Multi Layer Perceptron Markov Model. The results showed that the Multi Layer Perceptron Markov Model has performed the best. Praveen et al. (2013) investigated the applicability of a hybrid (CA-Markov) model in predicting LUCC in Saddle Creek drainage basin in Florida utilizing spatio-temporal data. Arsanjani et al., (2013) have developed a hybrid model consisting of logistic regression model, Markov chain (MC), and cellular automata (CA) to analyze the suburban expansion in the metropolitan area of Tehran, Iran for the years 2006, 2016, and 2026. The model was calibrated through comparing the actual and simulated land use maps of 2006 with a match of 89% being achieved. Sayemuzzaman and Jha (2014) combined the MC and CA techniques in order to integrate satellite-derived land cover maps of year 1992, 2001 and 2006 of North Carolina. Mondal et al., (2014) have used Landsat images of 1990 (TM), 2000 (ETM^+) and 2011 (LISS-III) for the classification and future LUCC prediction in a part of Narmada river of Madhya Pradesh. Supervised Fuzzy C-Mean classification was applied with overall accuracy of about 85 %. The MC was used for prediction with accuracy of about 92.5 %. Nurmiaty et al., (2014) have integrated CA and MC to assess land use change in Maros regency up to a 20 year period from Landsat images acquired in 2004, 2009, and 2012. Huang et al., (2015) have proposed a model for simulating LUCC based on MC and CA in the city of Wuhan, China. A spatial-temporal transition matrix was constructed from classified Landsat TM

images and then applied for simulating LUCC. The results showed the validity of the Markov-CA-based model for simulating urban LUCC. Han et al., (2015) combined a CLUE-S model with a Markov model to achieve a more realistic simulation of LUCC changes. Qiang and Lam (2015) used the transitional rules derived from ANN models in a CA model to simulate future LULC patterns. This paper proposes a method to improve the performance of the traditional MC model by running the model with multiple classifiers with different characteristics then combining the results by using the FMV. This is to accurately analyze LUCC trends, quantify the land cover losses and predict future LUCC scenarios in Delta, Egypt. After describing the study area in the following section, the methods are described, and then the results are presented and evaluated. Finally, the results are summarized.

2. Study area and Data Sources

The proposed study area for this research is located at Delta, Egypt. Delta plays a major role as a commercial and agricultural center as well as a provider of public services for its surrounding areas. The selected test area is located at 31°35′35″N, 31°04′54″E, on the northern coast of the Mediterranean Sea as shown in Figure 1. This area has increased potential to face massive erosion in future. To prepare the base maps for analysis and prediction purposes, Landsat satellite images for 2002, 2010 and 2015 have been collected from the official website of US Geological Survey (USGS) as shown in Table 1. Landsat Path 177 Row 38 covers the whole study area. Map Projection of the collected satellite images is the Universal Transverse Mercator (UTM)/ Zone 36N/ WGS-84 datum. Images from Landsat TM have seven bands with a spatial resolution of 30-120 m, while ETM images have eight spectral bands with a resolution of 15-30m. In order to resolve this problem, the lower resolutions (120m, 90m, and 60m) were resampled to higher resolution of 30m, which is enough to capture spatial details and small enough to reduce computation time (Bhatta et al., 2010). More details concerning the spectral ranges and spatial resolution of LANDSAT imagery can be referred to the *USGS* web site. The observation interval may differ because the cloud-free Landsat images are not available at a constant time interval (Figure 2).

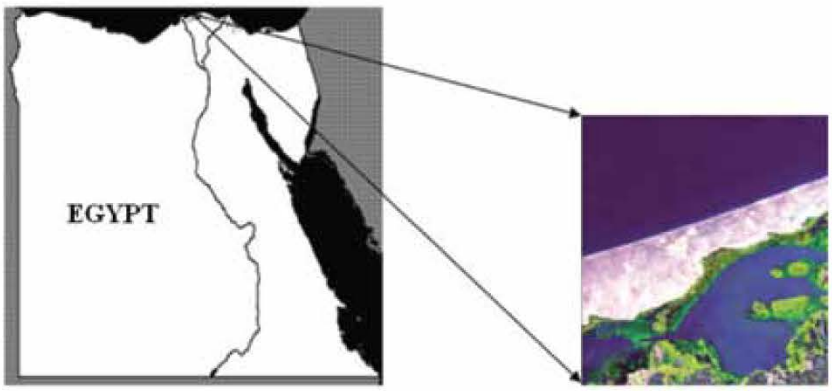

Figure 1: Geographical location of the study area - Delta, Egypt

Landsat-5 TM image (2002) Landsat-7 ETM+ image (2010) Landsat-7 ETM+ image (2015)

Figure 2: Landsat images of the study area - Delta, Egypt

Table 1: Details of the Landsat satellite images

Year	Acquisition Date	Sensor
2002	17/06/2002	Landsat-5 Thematic Mapper (TM)
2010	30/11/2010	Landsat-7 Enhanced Thematic Mapper (ETM+)
2015	09/09/2015	Landsat-7 Enhanced Thematic Mapper (ETM+)

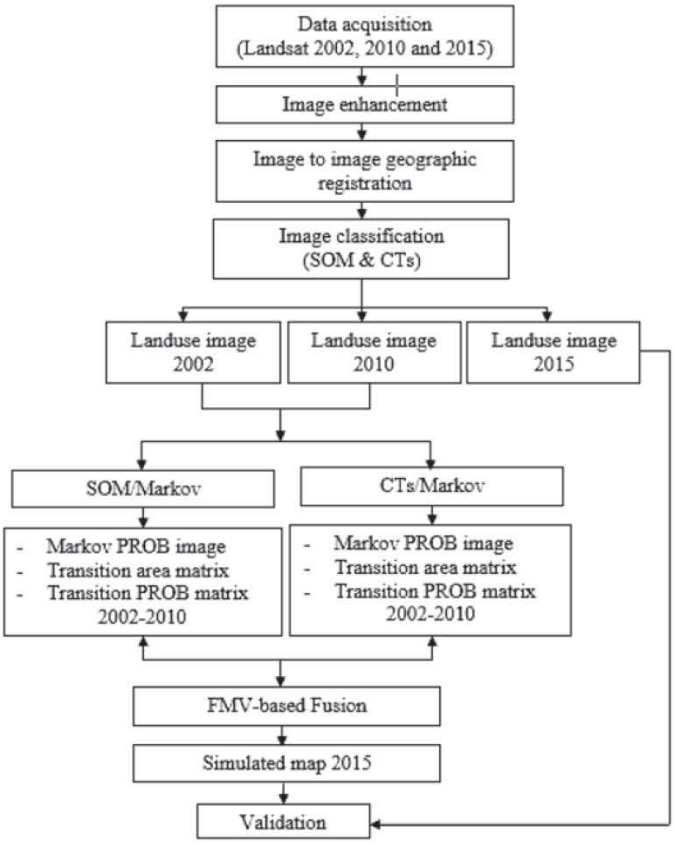

Figure 3: Flowchart of research method to improve the MC Model for future LUCC

3. Methodology

The primary objective of this research is to improve the performance of the MC Model for future LUCC prediction of a part of Delta, Egypt. The procedures used include: (i) acquisition and enhancement of Landsat images of 2002, 2010 and 2015; (ii) SOM and CTs-based classification of Landsat imagery; (iii) probability analysis using MC Model to generate LUCC maps of 2015 based on SOM and CTs results; (iv) FMV-based fusion of the Markovian probability; (vi) Validation of the predicted images of 2015. Figure 3 summarizes the methodology adopted in this study.

3.1 Data Preprocessing

3.1.1 Radiometric calibration and atmospheric correction

Each of the three satellite images was radiometrically and atmospherically corrected. Radiometric calibration of satellite data prior to classification and change detection from multi temporal image is necessary for gain and bias correction (Duggin and Robinove, 1990). The image derived Digital Number (DN) was converted back into at-sensor spectral radiance by calibrating the data using sensor calibration equation. A detailed description of the applied equations can be found in (Chander and Markham, 2003). Scattering effect is dominant for the Landsat data. Moreover, atmospheric correction is necessary for generation of auxiliary data (Song et al., 2001). Dark Object Subtraction (DOS) image based atmospheric correction model was adopted for correcting the VNIR bands due to its simplicity and non-availability of radio sounding data. As a result, radiance values were converted into atmospherically corrected reflectance (Chavez, 1996).

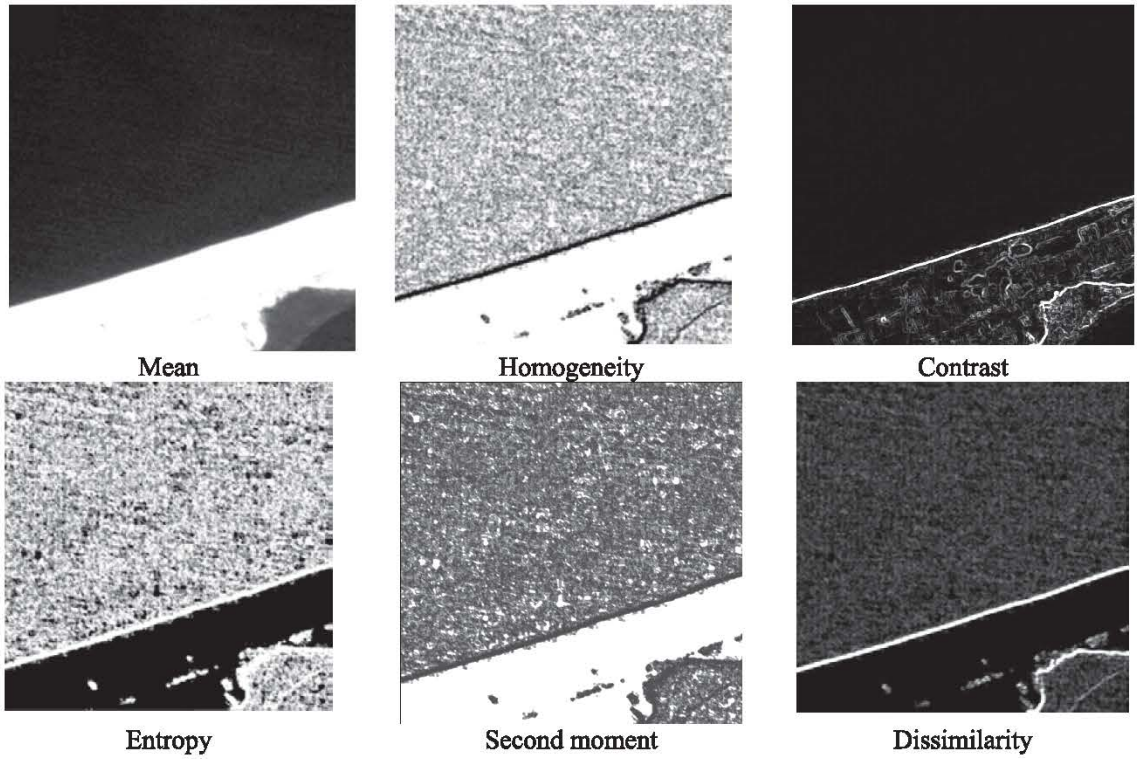

Figure 4: The full set of the possible GLCM attributes from the VNIR band

3.1.2. Generation of spectral attributes

Change detection based on post-classification comparison is negatively affected by classification errors of individual classified images. Contextual information has been incorporated in the classification process in order to mitigate the impacts of classification errors on change detection. Our experiments were carried out characterizing each pixel by an 11 element feature vector which comprises: 6 generated attributes, and the initial five bands of Landsat TM and ETM+. The six attributes include those derived from the Grey-Level Co-occurrence Matrix (GLCM) (Haralick, 1979) as shown in Figure 4. The attributes were calculated for the VNIR bands as input data for the two classifiers, SOM and CTs. These attributes have been selected to be uncorrelated based on the problem of correlation between feature attributes which has been studied in detail in Clausi (2002).

3.2 Land Cover Classification

In this work, the SOM and CTs classifiers have been used to prepare the land use maps of 2002, 2010 and 2015. Kanellopoulos et al., (1997) have demonstrated the complementary behaviors of neural and statistical algorithms in terms of classification errors. Therefore these classifiers result in uncorrelated classification errors and hence higher accuracies can then be reached by combining them. The initial five bands of Landsat TM and ETM+ and were considered for classification. Training pixels have been selected for each band of the input data as sets of manually classified samples. In order to evaluate the accuracy of the classifications undertaken in this research, reference data were captured by digitizing land areas; cultivated areas; and water bodies in the corrected imagery. SOM and CTs were then applied to generate these three major classes. Multiple sub-categories have been aggregated into one category in order to focus on the major land transition and eliminate errors among these sub-categories in the initial land use map (Pontius et al., 2010). After image classification, a 3 × 3 mode filter has been applied to generalize the classification results. This post-processing operation removes the isolated pixels which belong to one or more classes that differ from surrounding pixels and replaces these pixels to the most common neighboring class. As a final step, the position of the shoreline was adjusted to match the shoreline position when the mean high water (MHW) level is reached. The tide values were used to determine the maximum tide for each year by using the online tides and currents prediction website, http://tides.mobilegeographics.com. At each image acquisition date, the tide values were calculated.

After determining the MHW, plain surfaces were created to represent the higher tide for each year. Then by intersecting these surfaces with 30m SRTM data, www.glcf.umiacs.umd.edu/data/srtm, the intersection lines represented the maximum extent of the water inside the land area when the elevation of the water surface reached the maximum tide. Since the DEM was generated to the lands only and no bathymetric data were available, the extracted shorelines from satellite images and the maximum extent lines were intersect to define the shoreline at the MHW. After that, Google Earth was used to check and correct the interpreted images, which allowed obtaining the land use maps for 2002, 2010 and 2015.

3.2.1 Self-Organizing Map Classifier (SOM)

The SOM undertakes classification of imagery using Kohonen's SOM neural network (Kohonen, 2001). SOM requires no assumption regarding the statistical distribution of the input data and has two important properties: the ability to learn from input data; and to generalize and predict unseen patterns based on the data source. In this research, the SOM has 11 input neurons which are: 6 generated attributes and the initial five bands of Landsat TM and ETM+. The output layer of an SOM was organized as a 15 x 15 array of neurons as an output for the SOM (255 neurons). This number was selected because small networks result in some unrepresented classes in the final labeled network, while large networks lead to an improvement in the overall classification accuracy (Hugo et al., 2007). In the output of the SOM, each pixel is associated with a degree of membership for a certain class.

3.2.2 Classification Trees (CTs)

The theory of Classification trees was developed by Breiman et al., (1984). A CT is an iterative procedure in which a heterogeneous set of training data consisting of multiple classes is hierarchically subdivided progressively into more homogeneous clusters using a binary splitting rule to form the tree, which is then used to classify other similar datasets. CTs have the advantage that they work when the classification variables are a mixture of categorical and continuous. On the other hand, CTs is highly automatic since only the most prominent attributes are used in the final classification. The Entropy model (Shannon, 1949) was used as the splitting criteria in this study. Also, the trees were pruned through a 10-fold cross validation process, which has been demonstrated to produce highly accurate results. In the original output of the CTs, each pixel is associated with a degree of membership for the class at which particular leaf it was classified.

Accuracy assessments of the classification process were undertaken using Kappa statistics. The Kappa Index of Agreement (KIA) is a statistical measure adapted for accuracy assessment in Remote Sensing field by Congalton and Read (1983). KIA is a means to test two images, if their differences are due to 'chance' or 'real disagreement'. It is often used to check for accuracy of classified satellite images versus some 'real' ground-truth data.

3.3 Markov Chain (MC) Model

The MC model is commonly used to simulate LUCC based on the progression of the formation of Markov stochastic process systems (Muller and Middleton, 1994). It analyzes two qualitative land cover images of different dates and produces a transition area matrix, a transition probability matrix and a set of conditional probability images (Guana et al., 2011). The transition areas matrix represents the number of pixels that will be transformed over time from one land cover category to other categories. The matrix of transition probabilities shows the probability that each land cover category will change to other categories in 2015. This matrix is produced by the multiplication of each column in the transition probability matrix by the number of cells of corresponding land cover in the later image. The produced transition probability can be used to predict the probable land use change (Dadhich and Hanaoka, 2011). The prediction of future land use changes can be calculated as follows:

$$S(t+1) = p_{ij} * S(t)$$

Equation 1

$$P_{ij} = n_{ij} / \sum_{j=1}^{n} n_{ij} = \begin{pmatrix} P_{11} & P_{12} & P_{1n} \\ P_{21} & P_{22} & P_{2n} \\ P_{n1} & P_{n2} & P_{nn} \end{pmatrix}$$

Equation 2

$$(0 \leq PP_{ij} < 1 \text{ and } \sum_{j=1}^{N} P_{ij} = 1, (i, j = 1, 2, \ldots . n)$$

Equation 3

Where $S(t)$ represents the vector of land use at time t , $S(t+1)$ represents the vector of land use at time $(t+1)$, P_{ij} is the transition probability between i and j and n_{ij} denotes the number of transitions from i to j. This means that at any future period $t+k$, the matrix of cell transitions can be obtained by multiplying the vector of current land uses by the transition probability matrix P_{ij}, raised to the k^{th} power (P^k)

3.4 Fuzzy Majority Voting (FMV)-Based Combination of Markovian Probability

The idea is to give some semantics or meaning to the weights. Therefore, based on these semantics the values for the weights can be provided directly.

In the following the semantics based on fuzzy linguistic quantifiers for the weights are used. The fuzzy linguistic quantifiers were introduced by Zadeh (1983). For example, the membership function of relative quantifiers can be defined as (Herrera and Verdegay, 1996):

$$Q_{P_i} = \begin{cases} 0 & if\ pp_i < a \\ \dfrac{pp_i - a}{b - a} & if\ a \le pp_i \le b \\ 1 & if\ pp_i > b \end{cases}$$

Equation 4

With parameters a, b $\in$ [0, 1] and pp_i is the class membership of pixel i, Markovian probability in our case. Then, Yager (1998) proposed to compute the weights based on the linguistic quantifier represented by Q as follows:

$$w_{P_i} = Q_{P_i}\left(\frac{i}{N}\right) - Q_{P_i}\left(\frac{i-1}{N}\right),\ for\ i = 1\ ,\ .....\ ,N$$

Equation 5

Q_{P_i} is the membership functions of relative quantifiers, i is the order of the classifier after ranking Q_{P_i} for all classifiers in a descending order and N is the total number of classifiers. A relative quantifier 'at least half' with the parameter pair (0, 0.5) was applied for the membership function Q in equation 4. Then, depending on the total number of classifiers N, we can obtain from equation 5 the corresponding weighting vector $W = [w_1, ..., w_R]$. The final combined probability can be calculated as:

$$P_{FMV} = \arg\max_k \left[\sum_{i=1}^{N} w_{p_i}\ pp_i \right]$$

Equation 6

With w_{p_i} is the weight based on linguistic quantifier, pp_i is the Markovian probability of pixel i and k is the number of classes. For clarity, Table 2 is a typical example shows the calculations for one pixel.

3.5 Model Validation

Kappa coefficient was used to only validate the overall performance of the prediction process. However, this traditional method of validation, using Kappa statistics, is now out-of-date (Koomen, 2007). Therefore, it is of great important to validate the model output in an intelligent manner. For clarity, the validation process has been done by comparing three land use maps: 1) the land use map for 2010, 2) the land use map for 2015, and 3) the simulated the land use map for 2015. This three map comparison will allow one to distinguish the agreement due to correctly simulated persistence from the agreement due to correctly simulated change. The results are two components of agreement and three components of disagreement. The components of agreement are persistence simulated correctly and change simulated correctly. The components of disagreement are change simulated as persistence (the entries where reference 1 matches simulation but does not match reference 2), persistence simulated as change (the entries where reference 1 matches reference 2 but does not match simulation) and change simulated as change to wrong category (the entries where all three maps disagree). More details about these statistics can be found in Pontius et al. (2011). The present work was accomplished using a combination of the following software sets: 1) Erdas Imagine 9.2 for Data preprocessing, 2) IDRISI-Selva to calculate the transition probabilities and to prepare the base maps; and 3) a set of programs generated by the authors in Matlab environment for the fusion of Markovian probability maps.

Table 2: Combining Markovian probability based on FMV

Class	Markovian prob.		Q_{pp}		Q_{pp}`		w_{pp}`		P_{FMV}
	SOM/Markov	CTs/Markov	$Q1$	$Q2$	Q`1	Q`2	w_{pp}`1	w_{pp}`2	
L	0.2	0.4	0.4	0.8	0.8	0.4	0.4	0.2	0.2
C	0.1	0.3	0.2	0.6	0.6	0.2	0.3	0.1	0.1
W	0.1	0.1	0.2	0.2	0.2	0.2	0.1	0.1	0.0
Final class is L									

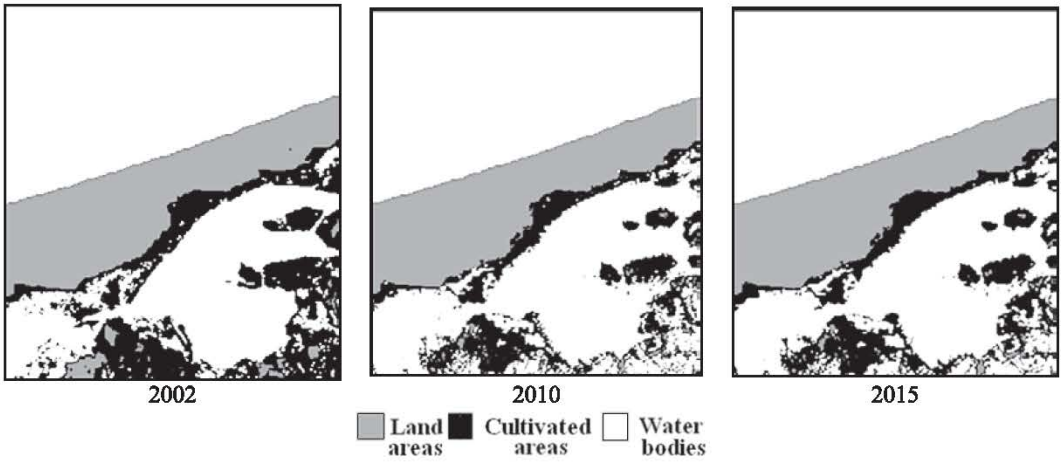

Figure 5: SOM land cover maps of the study area

Table 3: The overall KIA

	2002	2010	2015
SOM	0.8286	0.8249	0.8784
CTs	0.8894	0.8200	0.8277

Table 4: The per-class-KIA

	SOM			CTs		
	2002	2010	2015	2002	2010	2015
Land areas	0.9203	0.9096	0.8351	0.8045	0.9894	0.9656
Cultivated areas	0.7914	0.7441	0.8906	0.8567	0.7854	0.8151
Water bodies	0.8988	0.9984	0.9233	0.9894	0.8251	0.8251

4. Results and analysis

The experiment consisted of the validation and simulation phases. First, the 2015 LUCC map was simulated using the 2002 and 2010 datasets as the initial state, assuming that the transitional rules between 2002 and 2010 will continue during the next time interval. The 2015 LUCC simulated map was then compared with the 2015 LUCC classified map in order to evaluate the accuracy of the simulation process.

4.1 Land Use/Land Cover Classification

SOM and CTs were applied to generate three major classes. These classes along with their abbreviations are: land areas (L); cultivated areas (C); and water bodies (W). Figure 5 is a typical example shows SOM land cover maps for 2002, 2010 and 2015. The overall KIA of individual classifiers, based on the reference data, is given in Table 3. SOM performs slightly better with 0.8457 average overall KIA, followed by CTs with average overall KIA of 0.8440. On the other hand, the per-class-KIA for all the years is found ranging approximately from 0.7441 to 0.9984 as shown in Table 4.

4.2 Markov Chain (MC) Model

In order to predict the 2015 land use/cover map, the SOM and CTs-based classified images of 2002 and 2010 were applied as input data for the MC model. In this work, it is assumed that the factors that currently influence land use keep pace with the trend of LUCC change from 2002 to 2010 and will not have changed greatly from 2010 to 2015. For each classifier, a transition area matrix, a transition probability matrix and a set of conditional probability images have been obtained. For the rest of the paper, the SOM-based Markov model will be referred to as SOM/Markov, while the CTs-based Markov model will be referred to as CTs/Markov. Table 5, Table 6 and Figure 6 are typical examples of the results obtained for SOM/Markov. In Tables 5 and 6 the rows stand for the older land use/cover categories and the columns stand for newer land use/cover categories. Every cell of the diagonal, marked in grey, represents the probability for each category to undergo no change. The conditional probability images, Figure 6, show the possibility of transition to another land cover category. The transition probability matrix shows the transfer direction of land use types.

Table 5: Cells expected to transition to different classes in 2015

		Expected to transition to		
		Land	**Agricultural areas**	**Water bodies**
Cells in	Land	80665	2345	819
	Cultivated areas	2332	44016	12100
	Water bodies	110	5813	254789

Table 6: Markov probability of changing among land cover types in 2015

		Probability of changing to		
		Land	**Agricultural areas**	**Water bodies**
Given	Land	96.23	02.80	00.98
	Cultivated areas	03.99	75.31	20.70
	Water bodies	00.04	02.23	97.73

Markovian conditional prob. of being class 'L' | Markovian Conditional Prob. of being class 'C' | Markovian Conditional Prob. of being class 'W'

Figure 6: Markovian conditional probability images of 2015

Water bodies are the most stable class with 97.73% probability. The most dynamic class is the cultivated areas with transition probabilities of 75.31%. Cultivated land was primarily transformed into water bodies. This probabilistic prediction is dependent upon the past trend of the last eight years (2002-2010).

4.3 Future Prediction using MC Model

This step aims at producing one single land cover map for future prediction by combining the conditional probabilities obtained for SOM/Markov and CTs/Markov models based on FMV. The fused probability images, Obtained from the FMV, were then used to produce a single hard decision image by selecting the class image that contains the maximum probability and assigning that class to the output pixel. The predicted land cover map of 2015 is shown in Figure 7.

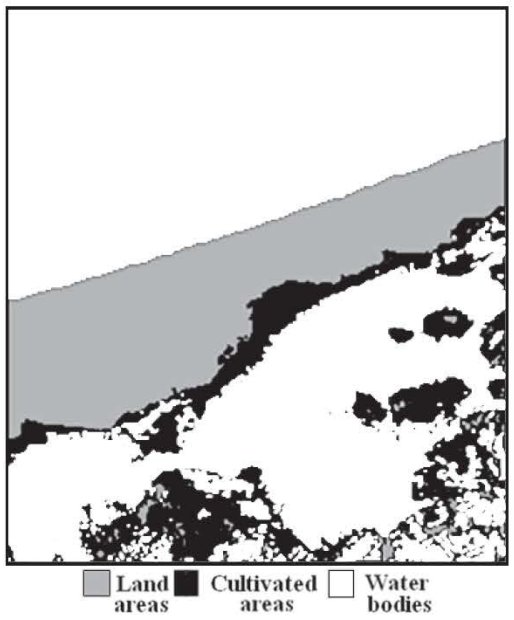

Figure 7: Final predicted land cover map for 2015 based on FMV fusion of SOM/Markov and CTs/Markov probabilities

Table 7: Overall KIA and per-class-KIA of the simulated images of 2015 as compared with the classified ones

	SOM/Markov	CTs/Markov	FMV Fusion
Land	0.6894	0.6409	0.8384
Cultivated areas	0.8854	0.7852	0.9040
Water bodies	0.8251	0.8644	0.9347
Overall KIA	0.8200	0.7854	0.8871

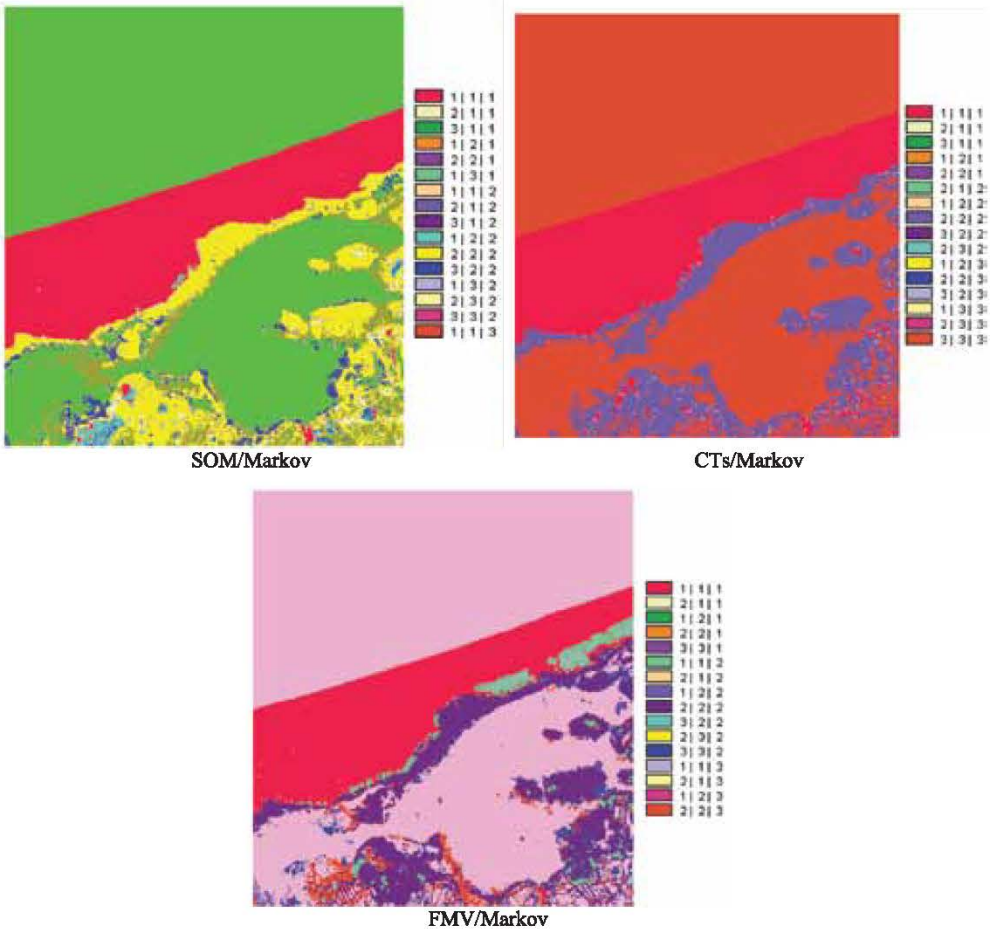

Figure 8: Maps of the components of agreement and disagreement between the reference 2015 map and the predicted one, '1': land areas, '2': cultivated areas, and '3': water bodies.

4. Model Validation

Model validation has been performed through the comparison of the simulated and classified maps of 2015. The comparison shows that the simulated map using FMV fusion is much more close to the reference one in 2015 than the simulated one using CTs/Markov and SOM/Markov. The overall KIA achieved for the prediction was about 0.7854, 0.8200 and 0.8871 for CTs/Markov, SOM/Markov and FMV fusion respectively, as shown in Table 7. The per-class-KIA of LUCC types for 2002, 2010 and 2015 has confirmed that the interpretation results met the analysis requirements. Figure 8 shows the spatial distribution of the components of agreement and disagreement.

The figure illustrates the pixels that correspond to each combination of categories in 2010, 2015 and simulated 2015 LUCC maps. For clarity, 2|3|3 refers to the pixels that have been transformed from category 2 (cultivated areas) in 2010 to category 3 (water bodies) in 2015, and have been simulated correctly. In terms of the percentages of disagreement and agreement components, table 8 shows that the total percentages of disagreement components are 24.42, 22.62 and 17.87% in the case of CTs/Markov, SOM/Markov and FMV fusion respectively. On the other hand, the total percentages of agreement components are 75.58, 77.38 and 82.13% for CTs/Markov, SOM/Markov and FMV fusion respectively.

Table 8: Ability of models to specify accurately components of agreement and disagreement

		SOM/Markov	CTs/Markov	FMV
components of agreement	persistence simulated correctly	59.90	58.56	62.28
	change simulated correctly	17.48	17.02	19.85
	Total agreement	**77.38**	**75.58**	**82.13**
components of disagreement	change simulated as persistence	7.68	7.02	5.70
	persistence simulated as change	10.29	12.16	8.77
	change simulated as change to wrong category	4.65	5.24	3.40
	Total disagreement	**22.62**	**24.42**	**17.87**

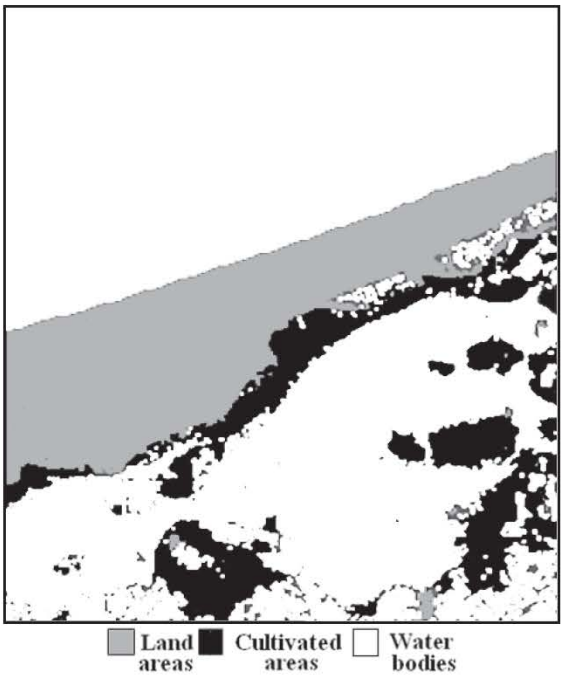

Figure 9: Simulated land cover map of Delta (2050)

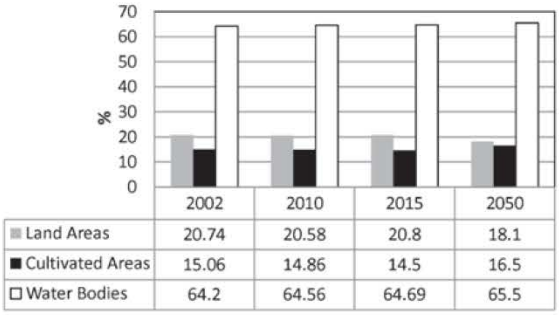

Figure 10: Percentages of presence of land cover types over the years (2002–2050)

4.5 Simulating the Land Cover Map of 2050

The prediction of 2050 land use was done to gain an idea about the future change. The base maps of 2002 and 2015 have been used to predict the land cover map of 2050 as shown in Figure 9. The predicted map of 2050 reveals that 65.50% of the total area will be occupied by water bodies. On the other hand, land areas are expected to cover approximately 18.10%, while cultivated areas will cover almost the remaining 16.50% types. As compared with 2015, Land use/cover map prediction of the test area for year 2050 shows 0.81% increase of water body. No systematic trend can be observed for land areas as well as for cultivated areas as shown in figure 10. One possible explanation is that the images collected for 2015 (September) and for 2002 (June) are from different seasons. This kind of variation might changes cultivated areas in one data set to land areas in other data sets and vice versa.

5. Conclusions

The future changes of Delta, Egypt have been predicted using Landsat satellite images of 2002, 2010 and 2015. SOM and CTs classification algorithms were used to prepare the base maps with three major classes: land areas; cultivated area; and water bodies. The classified images of 2002 and 2010 were used to predict the 2015 land use with a MC Model. The FMV was then applied for combining the measures of probability from the SOM/Markov and CTs/Markov models. The combined result was then validated with the 2015 classified image. The results show that the proposed model could simulate the LUCC changes of the test area with KIA of 0.8871 compared with 0.8200 for the best individual method, SOM/Markov.

The analysis of the Markov matrices suggests that combining probabilities from both SOM/Markov and CTs/Markov can be much more accurate and logical for predicting the future land cover changes. Based on the simulation scenario and by 2050, 65.50% of the total area will be occupied by water bodies. The findings could provide useful guidance for planning and management in the region. However, it is imperative that the Egyptian government provide a solution to this problem, so that Delta and its surrounding environments can be saved from more erosion in the future. For this research, Landsat images have been chosen that are freely available. The low resolution of 30 m is the main problem of working with Landsat images. IKONOS, QuickBird and WorldView or other satellite imagery with higher spatial resolution might be better option.

References

Arsanjani, J., Helbich, M., Kainz, W. and Boloorani, A., 2013, Integration of Logistic Regression, Markov Chain and Cellular Automata Models to Simulate Urban Expansion. *International Journal of Applied Earth Observation and Geoinformation*, 21 (2013): 265–275.

Atkinson, P.M. and Tatnall, A.L., 1997, Introduction Neural Networks in Remote Sensing. *International Journal of Remote Sensing*, 18: 699-709.

Bayes A. and Raquib A., 2012, Modeling Urban Land Cover Growth Dynamics Using Multi-Temporal Satellite Images: A Case Study of Dhaka, Bangladesh, *ISPRS International Journal of Geo-Information*, 1: 3-31.

Bhatta, B., Saraswati, S. and Bandyopadhyay, D., 2010, Quantifying the Degree-of-Freedom, Degree-of-Sprawl, and Degree-of-Goodness of Urban Growth from Remote Sensing Data, *Applied Geography,* 30: 96-111.

Breiman, L., Friedman, J. H., OLSHEN, R. A. and STONE, C. J. (editors), 1984, Classification and Regression Trees, Chapman & Hall, New York, 358 p.

Castella, J.C., Pheng Kam, S., Dinh Quang, D., Verburg, P.H. and Thai Hoanh, C., 2007, Combining Top-Down and Bottom-Up Modelling Approaches of Land Use/Cover Change to Support Public Policies: Application to Sustainable Management of Natural Resources in Northern Vietnam. *Land Use Policy 2007*, 24(3): 531–545.

Chander, G. and Markham, B., 2003, Revised Landsat-5 TM Radiometric Calibration Procedures and Post-Calibration Dynamic Ranges, *IEEE Geoscience and Remote Sensing Letters*, 41: 2674–2677.

Chavez, P. S., 1996, Image-Based Atmospheric Corrections Revisited and Improved; *Photogrammetric Engineering and Remote Sensing*, 62: 1025–1036.

Clark labs, 2012, http://www.clarklabs.org/applications/upload/land-change-modeler-IDRISI-focuspaper.pdf.

Clausi, D. A., 2002, An Analysis of Co-Occurrence Texture Statistics as a Function of Grey-Level Quantization. *Canadian Journal of Remote Sensing*, 28: 45-62.

Congalton, R. G. and Roy, A. M., 1983, A Quantitative Method to Test for Consistency and Correctness in Photointerpretation, *Photogrammetric Engineering and Remote Sensing*. 49(1): 69 – 74.

Dadhich, P.N., Hanaoka, S., 2011, Spatio-Temporal Urban Growth Modeling of Jaipur, India. *India Journal of Urban Technology*, 18:45–65.

De Chazal, J. and Rounsevell, M. D., 2009, Land-Use and Climate Change within Assessments of Biodiversity Change: A Review. *Global Environmental Change*, 19 (2): 306- 315.

Duggin, M. J. and Robinove, C. J., 1990, Assumptions Implicit in Remote Sensing Data Acquisition and Analysis; *International Journal of Remote Sensing*, 11: 1669–1694.

Eastman, J.R., 2009, IDRISI Taiga Guide to GIS and Image Processing; *Manual Version 16.02*; Clark Labs: Worcester, MA, USA, 2009.

El Raey, M., 1997, Vulnerability Assessment of the Coastal Zone of The Nile Delta of Egypt, to the Impacts of Sea Level Rise, *Ocean and Coastal Management,* 37: 29-40.

Gaber, A., Darwish, N., Sultan, Y., Arafat, S. and Koch M., 2014, Monitoring Building Stability in Port-Said City, Egypt Using Differential SAR Interferometry, *International Journal of Environment and Sustainability*, 3(1): 14-22.

Guana, D., Li, H., Inohaec, T., Su, W., Nagaiec, T. and Hokao, K., 2011, Modeling Urban Land Use Change by the Integration of Cellular Automaton and Markov Model; *Ecological Modelling,* 222(20): 3761–3772.

Han, H., Yang, C. Jinping Song, J., 2015, Scenario Simulation and the Prediction of Land Use and Land Cover Change in Beijing, China. *Sustainability*, 7(4): 4260-4279.

Haralick, R.M., 1979, Statistical and Structural Approaches to Texture, *Proceedings of the IEEE*, 67: 786–804.

Herrera, F. and Verdegay, J. L., 1996, A Linguistic Decision Process in Group Decision Making. *Group Decision Negotiation*, 5: 165-176.

Huang, J., Wu, Y., Gao, T., Zhan, Y. and Cui, W., 2015, An Integrated Approach based on Markov Chain and Cellular Automata to Simulation of Urban Land Use Changes. *Applied Mathematics and Information Sciences*, 9(2): 769-775.

Hugo, C., Capao, L., Fernando, B. and Mario, C., 2007, Meris Based Land Cover Classification with Self-Organizing Maps: preliminary results, *Proceedings of the 2nd EARSeL SIG Workshop on Land Use & Land Cover*, pp. 28-30.

Iacono, M., Levinson, D., El-Geneidy, A. and Wasfi, R., 2012, A Markov Chain Model of Land Use Change in the Twin Cities, 1958-2005, *Proceeding of the 10th International Symposium on Spatial Accuracy Assessment in Natural Resources and Environmental Sciences*, Florianopolis-SC, Brazil, pp. 345-350.

Joo, Y., Jun, C. and Park, S., 2010, Design of a Dynamic Land-Use Change Probability Model Using Spatio-Temporal Transition Matrix: Computational Science and Its Applications, *ICCSA 2010*, Volume 6016 of the series Lecture Notes in Computer Science, pp. 105-115.

Kanellopoulos, I., Wilkinson, G., Roli, F. and Austin, J. (editors), 1997, *Neurocomputation in Remote Sensing Data Analysis*, Springer, Berlin.

Kohonen, T., 2001, Self-Organizing Maps. Third Edition, Springer, New York.

Koomen, E. and Stillwell, J., 2007, Modelling Land Use-Change. in Koomen, E., Stillwell, J., Bakema, A., and Scholten, H. Modelling Land-Use Change, Volume 90 of the series The GeoJournal Library pp. 1-22.

LUCC (Land-Use and Land-Cover Change), 2002, www.geo.ucl.ac.be/LUCC/lucc.html

Mas, J. and Vega, E., 2012, Assessing Yearly Transition Probability Matrix for Land Use/Land Cover Dynamics. *Proceedings of the 10th international symposium on spatial accuracy assessment in natural resources and environmental sciences*, Florianopolis-SC, Brazil, July 10-13, 2012.

Mondal, A., Khare, D., Kundu, S. and Mishra, P., 2014, Detection of Land Use Change and Future Prediction with Markov Chain Model in a Part of Narmada River Basin, Madhya Pradesh. *Landscape Ecology and Water Management*, Part of the series Advances in Geographical and Environmental Sciences: 3-14.

Muller, M.R. and Middleton, J., 1994, A Markov Model of Land-Use Change Dynamics in The Niagara Region, Ontario, Canada. *Landscape Ecology*, 9(2):151–157.

Nurmiaty, S., Baja, S. and Arif, S., 2014, GIS-Based Modelling of Land Use Dynamics Using Cellular Automata and Markov Chain. *Journal of Environment and Earth Science*, 4(4), ISSN 2224-3216 (Paper) ISSN 2225-0948 (Online).

Pal, M. and Mather, P. M., 2004, Assessment of the Effectiveness of Support Vector Machines for Hyperspectral Data; *Future Generation Computer Systems* 20(7): 1215– 1225.

Pontius, J., Gilmore, R. and Petrova, S., 2010, Assessing a Predictive Model of Land Change using Uncertain Data. *Environmental Modeling and Software*, 25(3): 299-309.

Pontius, R.G., Peethambaram, S. and Castella, J.C., 2011, Comparison of Three Maps at Multiple Resolutions: A Case Study of Land Change Simulation in Cho Don District, Vietnam. *Annals of the Association of American Geographers*, 101(1): 45-62.

Praveen, S., Subedi, K. and Thapa, B., 2013, Application of a Hybrid Cellular Automaton Markov (CA-Markov) Model in Land-Use Change Prediction: A Case Study of Saddle Creek Drainage Basin, Florida. *Applied Ecology and Environmental Sciences*, 1(6): 126-132.

Qiang, Y. and Lam, N., 2015, Modeling Land Use and Land Cover Changes in a Vulnerable Coastal Region using Artificial Neural Networks and Cellular Automata. *Environmental Monitoring and Assessment*, March (2015): 187-57.

Sayemuzzaman, M. and Jha, M. , 2014, Modeling of Future Land Cover Land Use Change in North Carolina using Markov Chain and Cellular Automata Model. *American Journal of Engineering and Applied Sciences*, 7 (3): 292-303.

Shannon, C. E. (editor), 1949. Reprinted 1998, The Mathematical Theory of Communication, (Urbana, IL: University of Illinois Press), 324 p.

Song, C., Woodcock, C.E., Seto, K.C., Pax-Lenney, M. and Macomber, S. A., 2001, Classification and Change Detection using Landsat TM Data; *Remote Sensing of Environment*, 77: 241–246.

Stanley, D.J., 1988, Subsidence in the Northeastern Nile Delta – Rapid Rates, Possible Causes, and Consequences, *Science,* 240: 497–500.

Tewolde, M.G. and Cabral, P., 2011, Urban Sprawl Analysis and Modeling in Asmara, Eritrea. *Remote Sensing*, 3: 2148-2165.

Verburg, P.H., Eickhout, B. and Meijl, H.V., 2008, A Multi-Scale, Multi-Model Approach for Analyzing the Future Dynamics of European Land Use. *The Annals of Regional Science 2008*, 42(1): 57–77.

Wang, J. and Mountrakis, G., 2011, Developing a Multi-Network Urbanization (Munu) Model: A Case Study of Urban Growth in Denver, Colorado. *International Journal of Geographical Information Science*, *25*:229-253.

Wu, F., 2002, Calibration of Stochastic Cellular Automata: The Application to Rural-Urban Land Conversions, *International Journal of Geographical Information Science*, 16: 795-818.

Wu, F. and Webster. C. J., 2000, Simulating Artificial Cities in a GIS Environment: Urban Growth Under Alternative Regulation Regimes. *International Journal of Geographical Information Science*, 14 (7): 625–48.

Yager, R.R., 1998, On Ordered Weighted Averaging Aggregation Operators in Multicriteria Decision Making, *IEEE Transactions on Systems, Man, and Cybernetics*, 18: 183-190.

Zadeh, L. A., 1983, A Computational Approach to Fuzzy Quantifiers in Natural Languages, *Computers and Mathematics with Applications*, 9: 149-184.